



Anthroneamine based chromofluorogenic probes for Hg²⁺ detection in aqueous solution

Ashwani Kumar, Subodh Kumar*

Department of Chemistry, UGC-Center for Advance Studies, Guru Nank Dev University, Amritsar 143 005, India

ARTICLE INFO

Article history:

Received 6 December 2011

Revised 30 January 2012

Accepted 31 January 2012

Available online 14 February 2012

Keywords:

Fluorescence

Anthroneamine

Hg²⁺ chemosensor

Aqueous buffer

ABSTRACT

Anthroneamine derivatives **1–3** (H₂O:DMSO; 9:1, HEPES buffer, pH 7.0 ± 0.1) undergo highly selective fluorescence quenching with Hg²⁺. The observed linear fluorescence intensity change allows the quantitative detection of Hg²⁺ between 200 nM/40 ppb–12 μM/2.4 ppm even in the presence of interfering metal ions viz. Na⁺, K⁺, Mg²⁺, Ca²⁺, Ba²⁺, Cr³⁺, Fe²⁺, Co²⁺, Ni²⁺, Cu²⁺, Zn²⁺, Ag⁺, Cd²⁺, Pb²⁺. Probes **1–3** and their Hg²⁺ complexes also show the broad pH resistance for their practical applicability.

© 2012 Elsevier Ltd. All rights reserved.

The development of artificial chemosensors for both qualitative and quantitative recognition of environmentally and biologically important species is of great interest. In this regard, the chemosensors which can selectively sense the heavy metal ions such as mercury, lead, and copper are of great interest.¹ Mercury ions can easily pass through biological membranes and cause serious damage to the central nervous and endocrine systems.² Hg²⁺ ions are considered highly dangerous because both elemental and ionic mercury can be converted into methyl mercury by bacteria in the environment, which subsequently bio-accumulates through the food chain.³ So, considerable efforts have been made to synthesize the fluorescent chemosensors that can sense the mercury ions in a selective and sensitive manner under the physiological conditions.⁴

Among, the various molecular architectures, the thioether containing crown ethers/acetals,⁵ podands,⁶ thioureas,⁷ amines/amides,⁸ spirolactones,⁹ heterocycles based moieties¹⁰ etc. appropriately appended with chromogenic and fluorescent moieties have found applications in developing Hg²⁺ sensors. Most of these probes sense Hg²⁺ ion in a non-reversible (chemodosimeters) manner selectively and others in a reversible (chemosensors) manner usually non-selectively, and show some interference from either Cu²⁺/Ag⁺. The sensitivity of such types of probes is significantly affected by the percentage of water or effect of pH. Even though a few fluorescent Hg²⁺ probes with good water solubility, high selectivity and sensitivity are reported. As far as quantitative practical Hg²⁺ detection is concerned, a linear fluorescence response,

uniform fluorescence output at a broad pH range, compatibility with aqueous medium, higher selectivity, sensitivity, fast response and easy synthetic procedures of probes are most important. The Hg²⁺ probes reported so far have achieved only a few of the above mentioned criteria and do not satisfy all the desired features. So keeping in mind all these facts, new anthroneamine based probes **1–3** have been synthesized which show highly selective and sensitive reversible colorimetric and fluorescence behavior to Hg²⁺ ions under aqueous conditions (H₂O:DMSO; 9:1; HEPES buffer, pH 7.0 ± 0.1). The presence of electron-withdrawing bromine atoms on aromatic ring and alkyl chain on amide nitrogen tunes the sensitivity and pH applicability ranges of probes toward Hg²⁺ ions.

The commercially available 1-aminoanthracene-9,10-dione (**4**) on reaction with bromine in acetic acid at rt gave the respective dibromo derivative **5**, (98%), red solid, mp 240 °C. Compound **6** was obtained by heating 1-chloro-anthracene-9,10-dione with *n*-butylamine in DMSO. The stirring of suspension of **4–6** in acetonitrile with 2-chloroacetylchloride (2 equiv) at 45–50 °C in the presence of K₂CO₃ gave the respective 1-chloroacetamideanthracene-9,10-diones **7–9**, yellow colored solid, (>90%). The reaction of **7** with pyridine (2 equiv) in DMF on water bath for 6 h followed by hydrolysis with ethanol-morpholine mixture under reflux conditions gave yellowish-green solid **1** (85%)¹¹ (Scheme 1). Similarly, reactions of compounds **8** and **9** with pyridine followed by heating with ethanol-morpholine mixture gave respective probes **2**¹² and **3**¹³ in respective 60% and 85% yields. Probes **1–3** and intermediates were characterized using ¹H NMR, ¹³C NMR, IR, HRMS, and elemental analysis techniques. All the intermediate compounds and the final probes could be purified by crystallization and did not require column chromatography.

* Corresponding author.

E-mail address: subodh_gndu@yahoo.co.in (S. Kumar).

The presence of electron-withdrawing halogen atoms in probe **2** ($\lambda_{\text{max}} = 430 \text{ nm}$; $\epsilon = 10800$) causes hypsochromic shift of its electronic spectrum in comparison to that of probes **1** ($\lambda_{\text{max}} = 449 \text{ nm}$; $\epsilon = 11950$) and **3** ($\lambda_{\text{max}} = 450 \text{ nm}$; $\epsilon = 13100$). However, probes **1** and **2** on excitation at 435 nm show λ_{em} at 533 nm and 540 nm , respectively. Probes **1** and **3** have same high quantum yields ($\Phi = 0.53$), but probe **2** ($\Phi = 0.067$) probably due to the heavy atom effect of bromine atoms has a poor quantum yield.

Probe **1** ($20 \mu\text{M}$ H_2O : DMSO; (9: 1), HEPES buffer pH 7.0 ± 0.1), in its UV-vis spectrum showed absorbance maxima at 449 nm ($\epsilon = 11950$) which on addition of Hg^{2+} ions ($20 \text{ ppm}/100 \mu\text{M}$) underwent bathochromic shift at 522 nm associated with the naked eye visible color change from yellow-green to pink (Fig. 1). The addition of other metal ions viz. Na^+ , K^+ , Mg^{2+} , Ca^{2+} , Ba^{2+} , Cr^{3+} , Fe^{2+} , Co^{2+} , Ni^{2+} , Cu^{2+} , Zn^{2+} , Ag^+ , Cd^{2+} , Pb^{2+} even up to $200 \text{ ppm}/1 \text{ mM}$ did not show any change in the UV-Vis spectrum or color of the solution of probe **1**.

On gradual addition of aliquots of Hg^{2+} ions, the absorbance of probe **1** ($10 \mu\text{M}$, H_2O : DMSO (9:1); HEPES buffer pH 7.0 ± 0.1) at $\lambda_{\text{max}} = 450 \text{ nm}$ decreased gradually with concomitant increase in absorbance at 522 nm (Fig. 2a) and achieved a plateau above $12 \text{ ppm}/60 \mu\text{M}$ of Hg^{2+} with isobestic point at 500 nm . Spectral fitting of the absorbance data using the nonlinear regression analysis program SPECFIT-32 shows the formation of 1:1 stoichiometric complex with $\log \beta_{\text{ML}} = 5.18 \pm 0.06$. Ratiometrically probe **1** can detect Hg^{2+} ions from $1 \mu\text{M}$ to $60 \mu\text{M}$ in 90% aqueous buffered DMSO solution (Fig. 2b).

The addition of different metal ions, viz Na^+ , K^+ , Mg^{2+} , Ca^{2+} , Ba^{2+} , Cr^{3+} , Fe^{2+} , Co^{2+} , Ni^{2+} , Cu^{2+} , Zn^{2+} , Ag^+ , Cd^{2+} , Pb^{2+} to the solution of [**1**+ Hg^{2+} (5 equiv)] complex did not alter the absorbance intensity obtained for [**1**+ Hg^{2+} (5 equiv)] the complex and points that these metal ions do not interfere in the estimation of Hg^{2+} (Fig. S1 1). On excitation at 435 nm , probe **1** ($10 \mu\text{M}$, H_2O : DMSO (9:1), HEPES buffer pH = 7.0 ± 0.1) gave an emission band with $\lambda_{\text{max}} = 533 \text{ nm}$ ($\Phi = 0.53$), which on addition of Hg^{2+} ($4 \text{ ppm}/20 \mu\text{M}$) was quenched by >90%. Concomitantly, under illumination at 365 nm , the bright green solution of probe **1** became dark on addition of Hg^{2+} ions. The addition of other metal ions viz., Na^+ , K^+ , Mg^{2+} , Ca^{2+} , Ba^{2+} , Cr^{3+} , Fe^{2+} , Co^{2+} , Ni^{2+} , Cu^{2+} , Zn^{2+} , Ag^+ , Cd^{2+} , Pb^{2+} even up to $200 \text{ ppm}/1 \text{ mM}$ did not quench the fluorescence intensity of probe **1** (Figs. 3 and 5). Therefore, probe **1** recognizes only Hg^{2+} among various metal ions studied here.

Upon gradual addition of Hg^{2+} to **1** ($10 \mu\text{M}$, H_2O : DMSO (9:1), HEPES buffer pH 7.0 ± 0.1), the intensity of the emission band at $\lambda_{\text{max}} = 533 \text{ nm}$ decreased gradually with an increase in the concentration of Hg^{2+} (Fig. 4). The spectral fitting of the titration data shows the formation of 1:1 stoichiometric complex ($\log \beta_{\text{ML}} = 5.85 \pm 0.06$). For the practical quantitative detection, fluorescence spectral changes should vary linearly with the concentration of Hg^{2+} . A linear response of the fluorescence intensity as a function of [Hg^{2+}] was observed from $1\text{--}12 \mu\text{M}$ ($R = 0.997$) (inset Fig. 4).

The competitive experiments conducted in the presence of Hg^{2+} ($12 \mu\text{M}$) mixed with Na^+ , K^+ , Mg^{2+} , Ca^{2+} , Ba^{2+} , Cr^{3+} , Fe^{2+} , Co^{2+} , Ni^{2+} ,

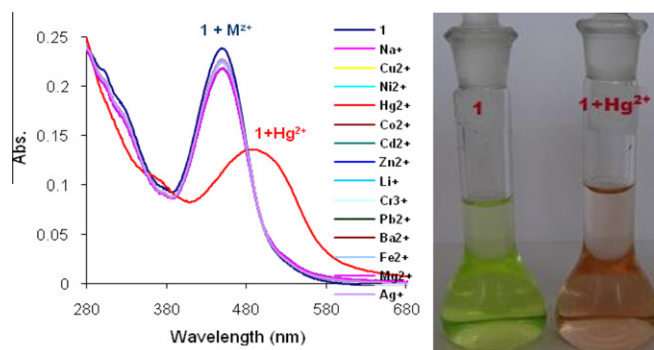


Figure 1. Effect of addition of Hg^{2+} and other metal ions on UV-vis spectrum and visible color change in **1** ($20 \mu\text{M}$, H_2O : DMSO (9:1), HEPES buffer (pH 7.0 ± 0.1)) on addition of Hg^{2+} .

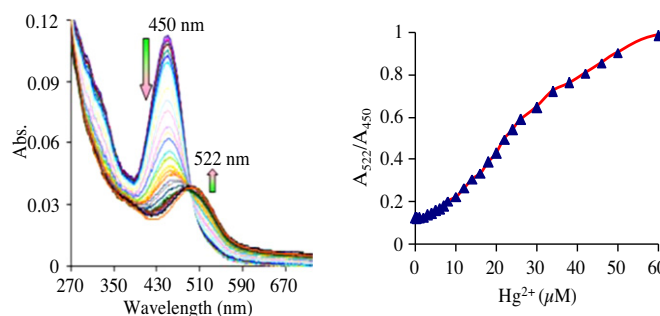


Figure 2. (a) Effect of gradual addition of Hg^{2+} ions on UV-vis spectrum of **1** ($10 \mu\text{M}$, H_2O : DMSO (9:1), HEPES buffer pH 7.0 ± 0.1). (b) Absorbance ratiometric response (A_{522}/A_{450}) of probe **1** ($10 \mu\text{M}$, H_2O : DMSO (9:1), HEPES buffer pH 7.0 ± 0.1) toward [Hg^{2+}].

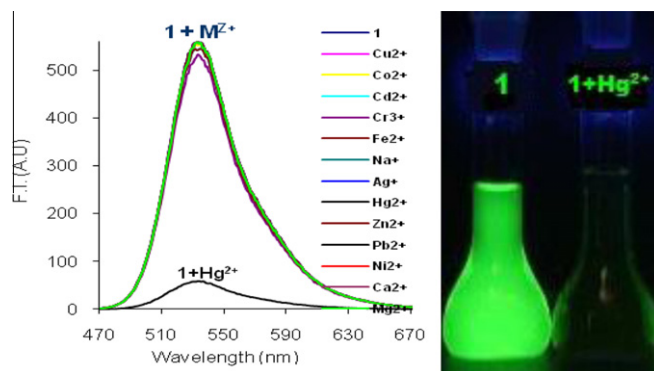
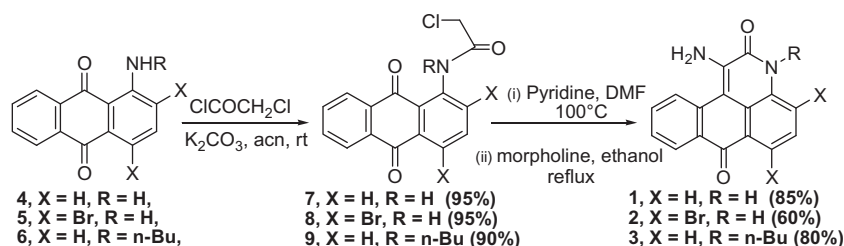


Figure 3. Effect of addition of Hg^{2+} and other metal ions on fluorescence spectrum and visible color change of **1** ($10 \mu\text{M}$, H_2O : DMSO (9:1), HEPES buffer pH 7.0 ± 0.1) under illumination at 365 nm .



Scheme 1. Synthesis of probes 1–3.

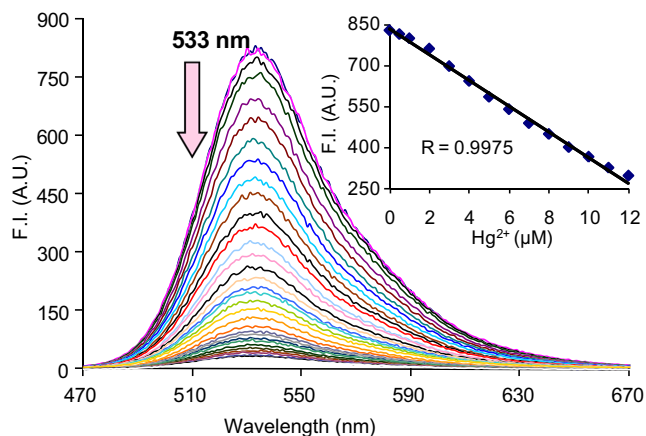


Figure 4. Effect of gradual addition of Hg^{2+} ions on the fluorescence intensity of **1** ($10 \mu\text{M}$, H_2O : DMSO 9:1, HEPES buffer pH 7.0 ± 0.1). Inset shows the linear relationship between FI and $[\text{Hg}^{2+}]$ (points refer to the experimental values).

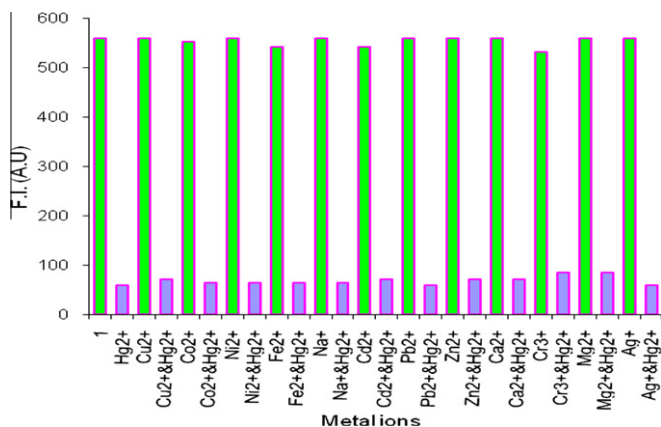


Figure 5. Effect of addition of individual metal ions and effect of interfering metal ions in presence of Hg^{2+} on the fluorescence intensity of probe **1** ($10 \mu\text{M}$, H_2O : DMSO (9:1), HEPES buffer pH 7.0 ± 0.1) (λ_{max} 533 nm).

Cu^{2+} , Zn^{2+} , Ag^+ , Cd^{2+} , Pb^{2+} (1 mM) show no significant variation in the fluorescence intensity in comparison with that observed by the addition of Hg^{2+} without the other metal ions (Fig. SI 2). These results point toward the highly selective recognition of Hg^{2+} and its applicability in the presence of other metal ions (Fig. 5). To examine further the reversibility of the processes, 10 equiv of EDTA was added to the solutions of probe **1** complexed with Hg^{2+} . The bright green fluorescence immediately turned on (fluorescence) and the yellow-green color (UV-vis. change) of the solution reappears (Fig. SI 3). This result implies the reversible character of binding of sensor **1** with Hg^{2+} .

Probe **2** ($20 \mu\text{M}$, H_2O : DMSO; 9:1, HEPES buffer pH = 7.0 ± 0.1), on gradual addition of Hg^{2+} ions showed gradual decrease in absorbance at λ_{max} 432 nm along with the formation of new absorption band at 515 nm (Figs. SI 4–6). The spectral fitting of these titration data shows the formation of only 1:1 stoichiometric complex ($\log \beta_{\text{ML}} = 5.18 \pm 0.18$). Probe **2** ($10 \mu\text{M}$, H_2O : DMSO; 9:1, HEPES buffer pH = 7.0 ± 0.1), on excitation at 435 nm gave emission band centered at 540 nm ($\Phi = 0.067$). On gradual addition of Hg^{2+} to the solution of **2**, the intensity of the emission band at λ_{max} 540 nm decreased gradually with increase in concentration of Hg^{2+} (Fig. 6). The spectral fitting of these titration data shows the formation of ML_2 and ML complexes ($\log \beta_{\text{ML}_2} = 13.31 \pm 0.24$, $\log \beta_{\text{ML}} = 6.85 \pm 0.10$). Linear decrease in fluorescence showed that probe **2** can detect Hg^{2+} ions in the range of 200 nM (40 ppb) – 4 μM (0.8 ppm).

Further in order to evaluate the role of amine NH_2 and amide NH in Hg^{2+} binding, probe **3** was synthesized. Probe **3** ($20 \mu\text{M}$, H_2O :DMSO; 9:1, HEPES buffer pH = 7.0 ± 0.1), where amidic NH of **1** has been converted to *N*-butyl moiety, on gradual addition of Hg^{2+} ions showed similar absorbance and emission spectral changes as shown by probe **1** (Figs. SI 7–9). These results clearly point that the *N*-alkylation of amidic N does not affect the Hg^{2+} recognition behavior of probe **1** and thus amine and amide carbonyl group mainly participate in Hg^{2+} recognition.

For the rapid monitoring of aqueous Hg^{2+} in environmental or biological samples, the fluorescence intensity should be resistant to changes in pH that may occur in unbuffered natural systems or in the analysis of samples from acidic or basic environments. The changes in the fluorescence intensity of probes **1–3** were monitored at solution pH values ranging 2–13, within which most biological samples can be tested. An analysis of pH induced changes in the fluorescence intensity of probe **1** shows that **1** undergoes deprotonation (monoanion) at $\text{pH} \geq 11$ and protonation at $\text{pH} \leq 4$ ($[\text{1.H}]^+$) both associated with fluorescence quenching. Therefore, probe **1** exists as a neutral molecule between pH ranges of 4–11 (Figs. SI 10–11). Similar analysis of pH induced changes in the fluorescence of probe **2** showed that it remains in the neutral form between pH 4–9 (Figs. SI 14–15). Probe **3**, due to the absence of amide NH moiety, showed enhanced basic pH stability as well as its practical applicability between the pH ranges of 4–12.5 (Fig. 7). Therefore, the protection of amide NH with *N*-butyl group stabilizes the probe over the broader pH range of 4–12 and the presence of electron-withdrawing bromo group in probe **2** facilitates the deprotonation of amide NH and thus affects their applicability over a relatively lower pH range of 4–9.

The fluorescence-pH titration of **1**- Hg^{2+} (1:10) complex also shows that probe **1** forms stable $[\text{1-Hg}^{2+}]^{2+}$ complex between pH 4–10 (Figs. SI 12–13) and probe **2** between pH 4–9.0 (Figs. SI 16–17). In the case of probe **3** enhanced stability of $[\text{3-Hg}^{2+}]$ complex between the broad pH range of 4–11.5 was observed (Fig. 8) (Figs. SI 20–21). The uniform activity over such a wide range of pH makes these molecules suitable for the analysis of environmental samples that would occur well within this extended range of pH, or for use in unbuffered medium.

So, substituents on the aromatic ring tune the sensitivity of the probes and the sensing range of 1–12 μM for probe **1** is further enhanced to 200 nM–4 μM for probe **2** upon the substitution of bromo group on aromatic ring. Whereas, alkylation of amidic nitrogen

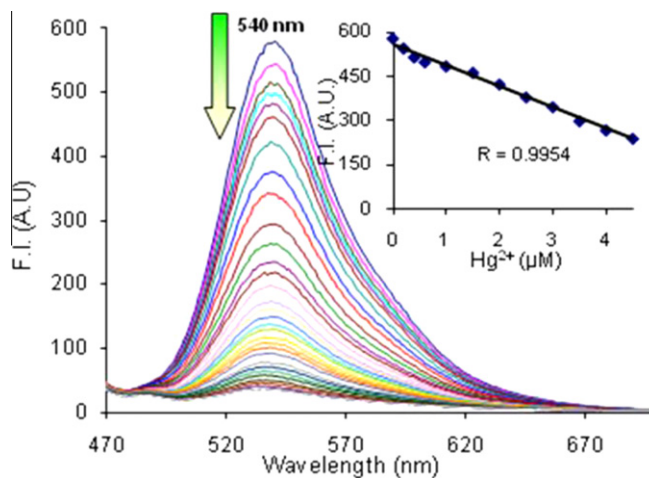


Figure 6. Effect of gradual addition of Hg^{2+} ions on the fluorescence intensity of **2** ($10 \mu\text{M}$, H_2O : DMSO (9:1), HEPES buffer pH 7.0 ± 0.1). Inset shows the linear relationship between FI and $[\text{Hg}^{2+}]$ (points refer to the experimental results).

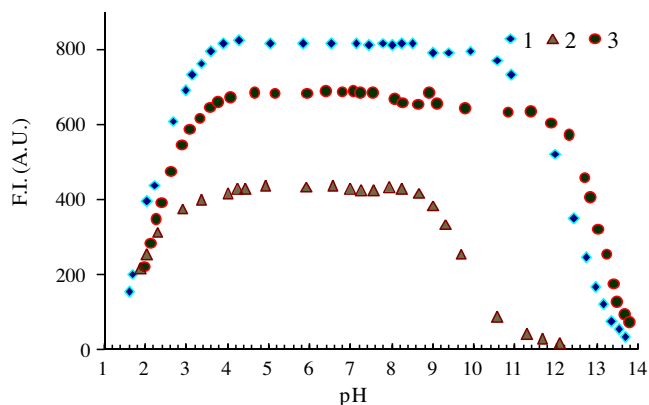


Figure 7. Effect of pH on fluorescence intensity of probes 1–3 (H₂O: DMSO (9:1), (points refer to the experimental results).

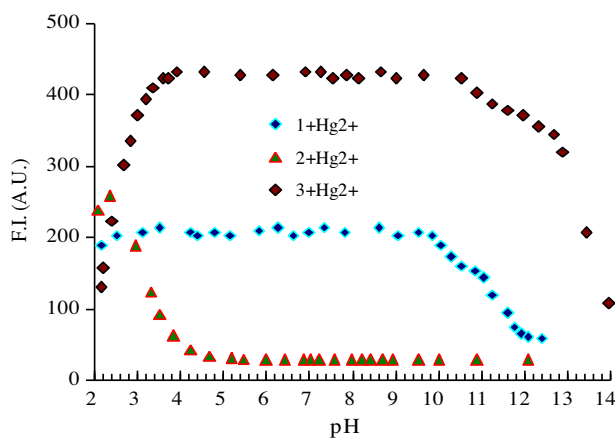


Figure 8. Effect of pH on fluorescence intensity of Hg²⁺ complexes of probes 1–3 (H₂O:DMSO (9:1)), (points refer to the experimental results).

tunes the pH range for the practical sensing of Hg²⁺ ions i.e. probe **1** can detect Hg²⁺ within the pH range of 4–10, and probe **3** with extended pH range of 4–11.5.

Thus, we have developed new anthroneamine based colorimetric and fluorescent probes **1–3** for selective and sensitive Hg²⁺ detection in aqueous medium. The ability of these probes to function in un-buffered aqueous solution with linear and fast fluorescence response will be useful for the rapid and quantitative detection of Hg²⁺ in environmental samples. Probes **1** and **3** find their applicability over a broad pH range of 4–12 with lowest detectable limits between 1 μM (0.2 ppm)–2 μM (0.4 ppm). The presence of electronegative bromine increases the sensitivity ten times for probe **2** toward Hg²⁺ with the lowest detection limit of 200 nM (40 ppb). Further, the effect of substituents and extension of aromatic ring to increase the sensitivity toward Hg²⁺ ions is in progress.

Acknowledgments

We thank DST, New Delhi for the financial assistance and FIST; UGC, New Delhi for CAS and fellowship to AK; CDRI Lucknow and the IISc Bangalore for mass spectra.

Supplementary data

Supplementary data associated with this article can be found, in the online version, at doi:10.1016/j.tetlet.2012.01.134.

References and notes

- (a) Gunnlaugsson, T.; Glynn, M.; Tocci, G. M.; Kruger, P. E.; Pfeffer, F. M. *Coord. Chem. Rev.* **2006**, *250*, 3094–3117; (b) Callan, J. F.; de Silva, A. P.; Magri, D. C. *Tetrahedron* **2005**, *61*, 8551–8588; (c) Kim, J. S.; Quang, D. T. *Chem. Rev.* **2007**, *107*, 3780–3799; (d) Kim, H. N.; Lee, M. H.; Kim, H. J.; Kim, J. S.; Yoon, J. *Chem. Soc. Rev.* **2008**, *37*, 1465–1472; (e) Carol, P.; Sreejith, S.; Ajayaghosh, A. *Chem. Asian J.* **2007**, *2*, 338–348; (f) Kaur, N.; Kumar, S. *Tetrahedron* **2011**, *67*, 9233–9264; (g) Quang, D. T.; Kim, J. S. *Chem. Rev.* **2010**, *110*, 6280–6301; (h) Jung, J. H.; Lee, J. H.; Shinkai, S. *Chem. Soc. Rev.* **2011**, *40*, 4464–4474.
- Gutknecht, J. *J. Membr. Biol.* **1981**, *61*, 61–66.
- (a) Boening, D. W. *Chemosphere* **2000**, *40*, 1335–1351; (b) Benoit, J. M.; Fitzgerald, W. F.; Damman, A. W. *Environ. Res.* **1998**, *78*, 118–133.
- (a) Lee, J. W.; Jung, H. S.; Kwon, P. S.; Kim, J. W.; Bartsch, R. A.; Kim, Y.; Kim, S.-J.; Kim, J. S. *Org. Lett.* **2008**, *10*, 3801–3804; (b) Nolan, E. M.; Lippard, S. J. *Chem. Rev.* **2008**, *108*, 3443–3480; (c) Lu, H.; Xiong, L.; Liu, H.; Yu, M.; Shen, Z.; Li, F.; You, X. *Org. Biomol. Chem.* **2009**, *7*, 2554–2558; (d) Mello, J. V.; Finney, N. S. *J. Am. Chem. Soc.* **2005**, *127*, 10124–10125; (e) Zhang, X.; Xiao, Y.; Qian, X. *Angew. Chem., Int. Ed.* **2008**, *47*, 8025–8029; (f) Lee, M. H.; Wu, J. S.; Lee, J. W.; Jung, J. H.; Kim, J. S. *Org. Lett.* **2007**, *9*, 2501–2504; (g) Zhou, Y.; Zhu, C.; Gao, Y. X.; You, X.; Yao, C. *Org. Lett.* **2010**, *12*, 2566–2569; (h) Ko, S.-K.; Chen, X.; Yoon, J.; Shin, I. *Chem. Soc. Rev.* **2011**, *40*, 2120–2130.
- (a) Voutsadaki, S.; Tsikalas, G. K.; Klontzas, E.; Froudakis, G. K.; Katerinopoulos, H. E. *Chem. Commun.* **2010**, *46*, 3292–3294; (b) Chen, T.; Zhu, W.; Xu, Y.; Zhang, S.; Zhang, X.; Qian, X. *Dalton Trans.* **2010**, *39*, 1316–1320; (c) Descalzo, A. B.; Martinez-Manez, R.; Radeglia, R.; Rurack, K.; Soto, J. *J. Am. Chem. Soc.* **2003**, *125*, 3418–3419; (d) Prodi, L.; Bargossi, C.; Montalti, M.; Zaccaroni, N.; Su, N.; Bradshaw, J. S.; Izatt, R. M.; Savage, P. B. *J. Am. Chem. Soc.* **2000**, *122*, 6769–6770; (e) Lioris, J. M.; Martinez-Manez, R.; Pardo, T.; Soto, J.; Padilla-Tosta, M. E. *Chem. Commun.* **1998**, 837; (f) Chen, Q.-Y.; Chen, C.-F. *Tetrahedron Lett.* **2005**, *46*, 165–168; (g) Tian, M.; Ihmels, H. *Eur. J. Org. Chem.* **2011**, *8*, 4145–4153; (h) Cheng, X.; Li, C.; Qin, J.; Li, Z. *Chem. Eur. J.* **2011**, *17*, 7276–7281; (i) Wanichacheva, N.; Setthakarn, K.; Prapawattananol, N.; Hanmeng, O.; Lee, V. S.; Grudpan, K. *J. Luminescence* **2012**, *132*, 35–40.
- (a) Kim, J. S.; Choi, M. G.; Song, K. C.; No, K. T.; Ahn, S.; Chang, S.-K. *Org. Lett.* **2007**, *9*, 1129–1132; (b) Ha-Thi, M.-H.; Penhoat, M.; Michelet, V.; Leray, I. *Org. Biomol. Chem.* **2009**, *7*, 1665–1673; (c) Sheng, R.; Wang, P.; Liu, W.; Wu, X.; Wu, S. *Sensors and Actuators B* **2008**, *128*, 507–511; (d) Youn, N. J.; Chang, S. K. *Tetrahedron Lett.* **2005**, *46*, 125–129; (e) Hsieh, Y.-C.; Chir, J.-L.; Wua, H.-H.; Chang, P.-S.; Wu, A.-T. *Carbohydr. Res.* **2009**, *344*, 2236–2239; (f) Chen, Y.-B.; Wang, Y.-J.; Lin, Y.-J.; Hu, C.-H.; Chen, S.-J.; Chir, J.-L.; Wu, A.-T. *Carbohydr. Res.* **2010**, *345*, 956–959; (g) Chen, K.-H.; Lu, C.-Y.; Cheng, H.-J.; Chen, S.-J.; Hu, C.-H.; Wu, A.-T. *Carbohydr. Res.* **2010**, *345*, 2557–2561.
- (a) Hennrich, G.; Sonnenschein, H.; ReschGenger, U. *J. Am. Chem. Soc.* **1999**, *121*, 5073–5074; (b) Mello, J. V.; Finney, N. S. *J. Am. Chem. Soc.* **2005**, *127*, 10124–10125; (c) Yang, H.; Zhou, Z.; Li, F.; Yi, T.; Huang, C. *Inorg. Chem. Commun.* **2007**, *10*, 1136–1139; (d) Yang, H.; Zhou, Z.-G.; Xu, J.; Li, F.-Y.; Yi, T.; Huang, C.-H. *Tetrahedron* **2007**, *63*, 6732–6736; (e) *Chem. Eur. J.* **2010**, *16*, 14424–14432. Near IR.; (f) Liu, Y.; Lv, X.; Zhao, Y.; Chen, M.; Liu, J.; Wang, P.; Guo, W. *Dyes and Pigments* **2012**, *92*, 909–915.
- (a) Wan, Y.; Niu, W.; Behof, W. J.; Wang, Y.; Boyle, P.; Gorman, C. B. *Tetrahedron* **2009**, *65*, 4293–4297; (b) Wang, J.; Qian, X. *Org. Lett.* **2006**, *8*, 3721–3724; (c) Wang, J.; Qian, X.; Cui, J. *J. Org. Chem.* **2006**, *71*, 4308–4311; (d) Mu, H.; Gong, R.; Ma, Q.; Sun, Y.; Fu, E. *Tetrahedron Lett.* **2007**, *48*, 5525–5529; (e) Lu, H.; Xiong, L.; Liu, H.; Yu, M.; Shen, Z.; Li, F.; You, X. *Org. Biomol. Chem.* **2009**, *7*, 2554–2558; (f) Chandrasekhar, V.; Pandey, M. D. *Tetrahedron Lett.* **2011**, *52*, 1938–1941; (g) Lohani, C. R.; Kim, J. M.; Lee, K.-H. *Tetrahedron* **2011**, *67*, 4130–4136.
- (a) Yang, Y.-K.; Yook, K.-J.; Tae, J. *J. Am. Chem. Soc.* **2005**, *127*, 16760–16761; (b) Yang, X.-F.; Lia, Y.; Bai, Q. *Analytica Chimica Acta* **2007**, *584*, 95–100; (c) Lin, W.; Cao, X.; Ding, Y.; Yuan, L.; Yu, Q. *Org. Biomol. Chem.* **2010**, *8*, 3618–3620.
- (a) Hu, J.; Zhang, M.; Yua, L. B.; Ju, Y. *Bioorg. Med. Chem. Lett.* **2010**, *20*, 4342–4345; (b) Ruan, Y.-B.; Maisonneuve, S.; Xie, J. *Dyes and Pigments* **2011**, *90*, 239–244; (c) Thomas, K. G.; Thomas, K. J.; Das, S.; George, M. V. *Chem. Commun.* **1997**, *6*, 597–598; (d) Basheer, M. C.; Alex, S.; Thomas, K. G.; Suresh, C. H.; Das, S. *Tetrahedron* **2006**, *62*, 605–610; (e) Liu, X.; Yang, X.; Peng, H.; Zhu, C.; Cheng, Y. *Tetrahedron Lett.* **2011**, *52*, 2295–2298; (f) Liu, X.; Yang, X.; Fu, Y.; Zhu, C.; Cheng, Y. *Tetrahedron* **2011**, *67*, 3181–3186.
- Anthroneamine (1)**: Dark yellow solid. Mp >250°C, HRMS (*m/z* +Na) = 285.0687, (Theoretical (*m/z* + Na) = 285.0640), IR ν_{\max} (KBr) 1595, 1635, 1671, 2857, 3305, 3422. ¹H NMR (DMSO-*d*₆ + CDCl₃, 300 MHz): δ 6.97 (s, 2H, NH₂), 7.47 (t, *J* = 7.8 Hz, 1H, ArH), 7.57 (t, *J* = 7.5 Hz, 1H, ArH), 7.65 (d, *J* = 7.8 Hz, 1H, ArH), 7.83 (t, *J* = 7.8 Hz, 1H, ArH), 8.16 (d, *J* = 7.8 Hz, 1H, ArH), 8.46 (d, *J* = 7.8 Hz, 1H, ArH), 8.64 (d, *J* = 8.1 Hz, 1H, ArH), 12.35 (s, 1H, NH); ¹³C NMR (CDCl₃+TFA, 75 MHz): δ 108.58, 112.37, 116.14, 119.82, 122.67, 125.82, 126.57, 127.02, 129.15, 129.66, 131.15, 135.05. Found: C, 73.31; H, 3.93; N, 10.72%. C₂₀H₁₈N₂O₂ requires C, 73.27; H, 3.84; N, 10.68%.
- 2,4-Dibromoanthroneamine (2)**: Dark brown solid. Mp >260 °C HRMS (*m/z* +Na) = 440.8844, 442.8924, 444.8894 (1:2:1), (Theoretical (*m/z* + Na) = 440.8850), IR ν_{\max} (KBr) 1590, 1664, 2855, 3033, 3162, 3405. ¹H NMR (DMSO-*d*₆, 300 MHz): δ 7.54–7.59 (doublet merged with broad NH₂ signal, 3H, 1ArH & NH₂), 7.79 (t, *J* = 7.8 Hz, 1H, ArH), 7.99 (s, 1H, ArH), 8.21 (d, *J* = 7.8 Hz, 1H, ArH), 8.49 (d, *J* = 8.1 Hz, 1H, ArH), 9.78 (s, 1H, NH). ¹³C NMR (DMSO-*d*₆, 75 MHz): δ 103.06, 112.74, 115.27, 117.42, 122.53, 122.79, 125.96, 126.90, 127.40, 128.31, 131.41, 133.11, 133.50, 139.32, 157.99, 180.56. Found: C, 45.82; H, 1.98; N, 6.72%. C₂₀H₁₈N₂O₂ requires C, 45.75; H, 1.92; N, 6.67%.

13. *N*-Butylanthrone amine (**3**): Yellow needle like crystalline solid. Mp = 118 °C, HRMS (m/z +Na) = 341.1268, (Theoretical (m/z +Na) = 341.1266), IR ν_{max} (KBr) 1581, 1649, 2866, 3329. ^1H NMR (CDCl_3 , 400 MHz): δ 1.04 (t, J = 7.2 Hz, 3H, CH_3), 1.52–1.57 (m, 2H, CH_2), 1.82–1.84 (m, 2H, CH_2), 4.46 (t, J = 7.6 Hz, 2H, CH_2), 5.94 (s, 2H, NH_2), 7.56–7.58 (m, 2H, 2 \times ArH), 7.62 (t, J = 8.4 Hz, 1H, ArH), 7.77 (d, J = 8.4 Hz, 1H, ArH), 8.36 (d, J = 8.4 Hz, 1H, ArH), 8.53 – 8.59 (m, 2H, 2 \times ArH); ^{13}C NMR (CDCl_3 , 100 MHz): δ 13.77, 20.39, 30.02, 43.73, 107.12, 118.24, 121.12, 123.36, 125.75, 127.79, 128.29, 128.86, 132.08, 132.57, 133.22, 135.77, 137.07, 158.65, 182.56. Found: C, 75.31; H, 5.81; N, 8.85%. $\text{C}_{20}\text{H}_{18}\text{N}_2\text{O}_2$ requires C, 75.45; H, 5.70; N, 8.80%.